



Valorization of waste mill tailings from small-scale mining through geopolymerization: strength, durability, and heavy metal leaching potential

Christian R. Orozco¹ · Kim Deirdre Lynn T. Castro¹ · Ma. Mikaela T. De Boda¹

Received: 8 August 2022 / Accepted: 19 February 2023 / Published online: 2 March 2023
© The Author(s), under exclusive licence to Springer-Verlag GmbH Germany, part of Springer Nature 2023

Abstract

Purpose Mill tailings are sediments produced after the metal-bearing mineral has been separated from an ore's uneconomic fraction. These residues are disposed to tailings dams that are costly, occupy large land areas, and may cause environmental and safety problems. This study aims to use this waste to produce a construction material by geopolymerization, an environment-friendly process that uses less energy and gives products comparable strength and long-term durability.

Materials and method We produced bricks from contaminated gold mill tailings using geopolymerization. The varied parameters are the alkali activator (NaOH and Ca(OH)₂), forming pressure (0.03 and 1.78 MPa), curing temperature (60 and 80 °C), and curing age (7 and 28 days). We evaluated the geopolymer bricks' compressive strength and durability for mechanical performance. For environmental performance, we compared the leaching of heavy metals (arsenic, copper, cadmium, chromium, lead, and mercury) in the raw mill tailings and geopolymerized bricks. We used statistical analyses to investigate the interaction of factors affecting performance of the geopolymer bricks.

Results and discussion Physical and chemical characterization results of gold mill tailings show that it is a material suitable for geopolymerization. Most geopolymer samples generated unconfined compressive strength acceptable for pavement subbase applications. Samples have shown high heavy metal immobilization rates of 33.35–100% and have passed the US Environmental Protection Agency (EPA) limits on As, Cu, Cd, Cr, Pb, and Hg. Durability analysis showed different outcomes depending on the reactions of the alkali-activator as a base to the sulfuric acid bath. Mass loss and mass gain were observed for NaOH and Ca(OH)₂ geopolymer samples, respectively.

Conclusion This work has shown that contaminated mill tailing sediments can be used as construction material through geopolymerization based on mechanical properties and environmental performance.

Keywords Geopolymerization · Heavy metals · Mill tailings · Mining · Statistical analysis

1 Introduction

The gold extraction process from small-scale mining yields pulverized rock by-products called mill tailings (Behera et al. 2021). These residues are disposed to be dewatered and pumped to the tailings pond or dam (Qian et al. 2023). Tailings are materials, whether solid, liquid, or a combination of the two, that are separated from the ores during the

milling and concentration processes (Qaidi et al. 2022b). They are pulverized rocks with no monetary value that remain after the ore is processed to extract the economically valuable and metal-bearing minerals (Brockenbrough and Editor 2009). Each year, more mill tailings are produced because of the growing number of small-scale mining operations in the Philippines and many other middle-income countries (Macasieb et al. 2021a; Opiso et al. 2021). As a result, existing tailings dams will eventually be unable to handle any additional waste. Therefore, alternative waste disposal methods that are both environmentally and economically viable must be developed and explored.

Indiscriminate mill tailings disposal poses a threat to the environment and human health (Qaidi et al. 2022b) since they contain leftover processing chemicals, such as heavy

Responsible editor: Jos Brils

✉ Christian R. Orozco
croszco@up.edu.ph

¹ Institute of Civil Engineering, University of the Philippines Diliman, Quezon City, Philippines

metals (Cairncross and Tadie 2022), from the gold extraction process. Disposal of these wastes in tailings dams or ponds may cause surface water, groundwater, and soil contamination (Macasieb et al. 2021b). Tailings dams are also vulnerable to erosion, collapse (Silva Rotta et al. 2020), and heavy metal leaching (Shi et al. 2023). Moreover, this type of disposal facility is costly (Cox et al. 2022) and occupies large areas of land (Ahmari and Zhang 2013). A number of different methods have been applied for the disposal of mill tailings due to environmental pressure and economic factors. One of the most common means of mill tailings disposal is through tailings ponds or dams typically built close to the mining site (Adiansyah et al. 2015). In this method, the underlying ground must be structurally sound and carry the catchment's weight. Kesimal et al. (2004) studied mine tailings as backfill material in mining sites. The mine tailings were mixed with water and cement or other pozzolanic binder material to increase the strength properties of the tailings. Ordinary Portland cement is the most used binder material in this method (Behera et al. 2021). However, the quantity of mill tailings produced is enormous, and not all tailings can be utilized as backfill material. This leads to more interest in finding other ways of utilizing this mining waste in the construction industry (Kiventerä et al. 2016).

Studies on more economical and environmentally friendly alternatives for waste mill tailing disposal have emerged in the recent decade. Among these, geopolymerization has sparked the interest of many researchers in the construction sector (Nawaz et al. 2020; Sheikhhosseini Lori et al. 2021; Qaidi et al. 2022b) since it is an eco-friendly process (Xiaolong et al. 2021) that requires low cost and low power consumption (Zhang 2013). At the same time, this process produces materials with strength acceptable for various construction applications (Ahmari and Zhang 2014; Sheikhhosseini Lori et al. 2021). Geopolymerization is the chemical reaction of aluminosilicate-rich solids in a highly concentrated alkali hydroxide or silicate solution (Xiaolong et al. 2021). In this process, a stable material called geopolymer with amorphous polymeric structures with interconnected Si–O–Al–O–Si bonds is formed (Zhang et al. 2011). As a stabilizing process, geopolymerization has been proven to have lower carbon footprint production than standard ordinary Portland cement (Petrillo et al. 2016). Geopolymer soils have also been viewed to have metal ion adsorbents or catalysts (Tian and Sasaki 2021). For stabilizing soils, geopolymerized brick samples can have different uses, depending on the results of their strength and durability. They can be used as a structural clay load-bearing wall tile, building brick, solid masonry unit, or light traffic paving brick sample (Zhang 2013).

Using bricks from geopolymerization depends on the properties of the final product. Compressive strength and durability are essential properties in construction that

determine a particular material's use (Corpuz et al. 2021; Orozco and Urbino 2022). Various factors affect these performance indicators, including the type of activator (Li et al. 2022), forming pressure (Ahmari and Zhang 2013), and curing condition (Saif et al. 2022; Qaidi et al. 2022a). Different activators have been used for producing geopolymers (Leong et al. 2018). Zhang et al. (2011) reported that high NaOH alkali-activator concentration dissolves more alumina and silica components, producing a thicker geopolymeric binder, thus resulting in higher strength. In the study of Khater (2012), he found that adding calcium to the geopolymer systems improves their ability to harden at ambient temperature. Curing temperature is an essential factor in the geopolymerization process (Tayeh et al. 2021) using mine or mill tailings because of the raw material's low reactivity compared to other source materials. Curing temperature greatly affects the strength development of geopolymer samples (Amin et al. 2021). A higher temperature of 40 to 95 °C is needed to form a sufficiently interconnected network of bonds within the geopolymer (Abdullah et al. 2015). Curing time or age influences the compressive strength and the water absorption of the specimen. A longer curing age gives the three-dimensional geopolymeric framework more time to sufficiently form, leading to higher strength development. In the study of Jallu et al. (2021) for fly ash (FA) geopolymer, higher strength development at longer age was attributed to the consumption of pozzolanic ions and the degree of hydration in FA geopolymer with curing time. However, for some specimens, a long curing period produces strength that does not vary significantly from those cured for a short period (Sindhunata et al. 2006). The limited improving effect of forming pressure has been studied by Freidin (2007). His study observed that the rate of increase in strength with the forming pressure decreases as the forming pressure increases. Forming pressure causes the particles of the geopolymer paste to rearrange to a denser configuration pushing the air out and filling the voids in the matrix, reducing its porosity and yielding higher compressive strength (Bai et al. 2022).

The general objective of this study is to produce bricks (geopolymer specimens) composed of gold mill tailings from a small-scale mining operation by geopolymerization. Various factors (alkali-activator, curing temperature, and forming pressure) affecting the performance (strength, durability, and leaching potential) of geopolymerized mill tailings were investigated. This study will add value to this waste material and provide an eco-friendly and cost-effective manufacturing method. It will contribute to limited studies on using geopolymerization as a sustainable process of utilizing waste mill tailings from small-scale mining industries. In addition, countries with similar issues on sustainable utilization of this waste material will benefit from this study.

2 Materials and methods

2.1 Physico-chemical characterization of mill tailings

The present study utilized gold mill tailings (MT) sourced from a small-scale mining facility located in Itogon, Benguet, Philippines. The raw MT samples, weighing a total of 40 kg, were collected and characterized as saturated sandy soil. The physical properties of the mill tailings, including particle size distribution and Atterberg limits, were determined through standard testing procedures. Particle size analysis was conducted in accordance with the American Society for Testing and Materials (ASTM) D422-63 Standard Test Method for Particle-Size Analysis of Soil (ASTM 2014). Furthermore, the liquid limit and plastic limit were determined in accordance with ASTM D4318-0 Standard Test Methods for Liquid Limit, Plastic Limit, and Plasticity Index of Soils in order to classify the raw MT samples (Haigh 2016).

Aluminosilicate materials are essential in strength development and other properties associated with geopolymers. Thus, to identify minerals present in the mill tailings used in the study, chemical characterization was done by X-ray diffraction (XRD) analysis. The XRD analysis was performed with the MAXima XRD-7000 Shimadzu. First, the mineralogy was evaluated and checked manually using Mineral Database (Materials Data Inc., 1988–2004). Then, these values were cross-referenced to an existing database of minerals on ruff.info and their corresponding diffraction patterns to identify the minerals present in the mill tailings. The detection limit is 5% and is strongly dependent on crystallinity.

2.2 Test cases and sample preparation

A preliminary experiment (trial mix) was performed to determine the actual geopolymer mix-design test cases. Previous studies (Zhang et al. 2011; Abdullah et al. 2015; Freidin 2007) were considered for developing the test cases. The selection of the most consistent geopolymer paste was based on the results of trial mixes. The consistency of the geopolymer pastes was observed to be optimal at a 0.3 ratio for the 10 M NaOH solution and 0.6 ratio for the 10 M Ca(OH)₂ solution. The total number of samples prepared for testing and the corresponding preparation and testing conditions are presented in Table 1. For each test case, three samples were prepared, and the actual geopolymer specimens are illustrated in Fig. 1.

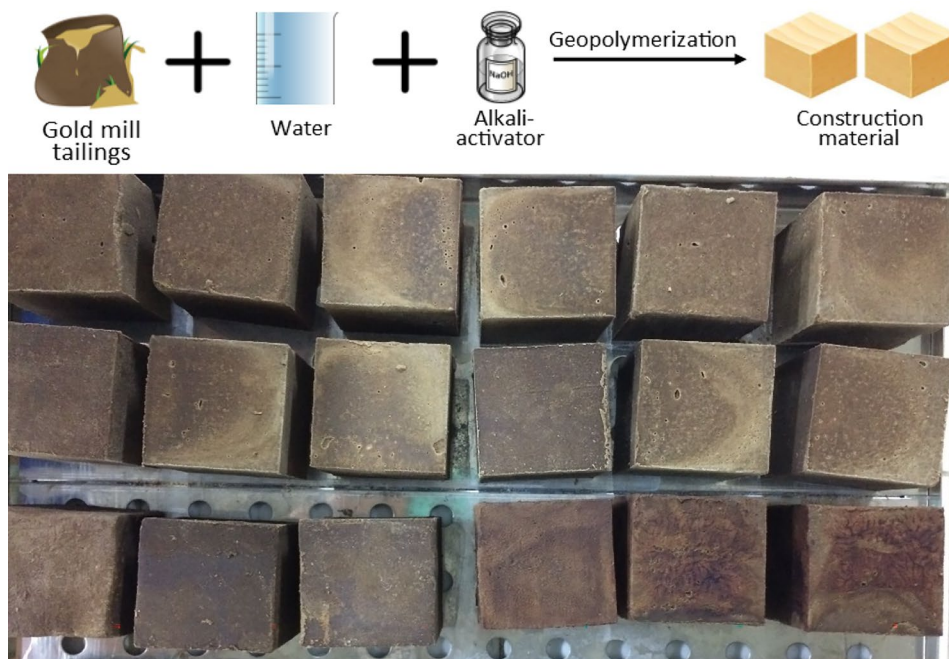
The alkali activators used were reagent-grade sodium hydroxide (NaOH) pellets with a purity of 99% and reagent-grade calcium hydroxide (Ca(OH)₂) with a purity of 95%. Ten molar solutions of both alkali activators were prepared. To prepare the 10 M NaOH solution, 400 g of NaOH pellets (with a molar mass of 40 g/mol) were dissolved in 1 L of water. The 10 M Ca(OH)₂ solution was prepared by adding 740 g of Ca(OH)₂ powder (with a molar mass of 74 g/mol) to 1 L of water. The solutions were thoroughly mixed and stored for use in the production of geopolymer samples.

The raw gold mill tailings used in the study were dried in an oven at 110 °C for 24 h and sieved at sieve no. 16 (1.19 mm opening diameter) to ensure uniformity. For each geopolymer specimen, 200 g of mill tailings were utilized. In a test case with three replicates, 1.2 kg of mill tailings were mixed with 360 and 720 g of 10 M NaOH solution and 10 M Ca(OH)₂

Table 1 Treatment conditions of geopolymer samples

Sample	Alkali activator (ratio)	Forming pressure	Curing temperature	Curing time (day)	No. of samples
A1	10 M NaOH (0.3)	0.03 MPa	60 °C	7	3
A2				28	9
B1		1.78 MPa	80 °C	7	3
B2				28	9
C1		0.03 MPa	60 °C	7	3
C2				28	9
D1		1.78 MPa	80 °C	7	3
D2				28	9
E1	10 M Ca(OH) ₂ (0.6)	0.03 MPa	60 °C	7	3
E2				28	9
F1		1.78 MPa	80 °C	7	3
F2				28	9
G1		0.03 MPa	60 °C	7	3
G2				28	9
H1			80 °C	7	3
H2				28	9

Fig. 1 Overview of geopolymerization process (top) and actual samples of geopolymer bricks from mill tailings (bottom)



solution, respectively. The mixing was performed using a mechanical mixer for 10 min to attain the desired geopolymer paste. The geopolymer paste was then carefully placed in molds in three layers, compressing each layer to eliminate voids. Subsequently, forming pressure was applied, with two pressures varied in the study: 0.03 and 1.78 MPa. The geopolymer paste was allowed to set in the mold for a minimum of 8 h before demolding and placement on pans. The specimens were then heat cured in an oven at 60 and 80 °C for 24 h and allowed to age under ambient temperature until testing at 7 and 28 days to achieve strength development.

2.3 Unconfined compressive strength test

The compressive strength of the geopolymer samples was determined using a Universal Testing Machine (UTM). Geopolymer specimens were subjected one at a time to compression using UTM after seven days and 28 days of curing at ambient temperature. A constant loading rate of 0.5 mm/min was applied for all specimens until failure. All crushed specimens were stored in zipper storage bags for subsequent testing of heavy metal leaching potential.

2.4 Durability test

The durability performance of the geopolymer samples was evaluated through a static acid immersion test, as described by Davidovits (2002). The procedure involved immersing the geopolymer samples in a strong sulfuric acid solution (5% H₂SO₄) for 28 days. The samples were placed in a container containing the acid bath, and after 28 days, they were

removed and their final masses were recorded. The mass loss of the geopolymer specimens in a corrosive environment is an indication of their durability.

2.5 Leaching potential test

The heavy metal leaching potential of the geopolymer samples was assessed using the toxicity characteristic leaching procedure (TCLP). This test was performed in accordance with the United States Environmental Protection Agency (US EPA) Test Method 1311 to evaluate the ability of the geopolymer samples to immobilize heavy metals present in the raw gold mill tailings. The crushed geopolymer specimens, obtained after the unconfined compression test, were subjected to the TCLP extraction process. The leached heavy metals were analyzed using inductively coupled plasma–optical emission spectroscopy (ICP-OES) to determine the effectiveness of the geopolymer samples in immobilizing heavy metals.

3 Results and discussion

3.1 Physico-chemical characteristics of mill tailings

The gradation curve from sieving the mill tailings sample shows a well-graded material. Further classification was conducted in accordance with the Unified Soil Classification System (USCS). ASTM D2487-10 Standard Practice for Classification of Soils for Engineering Purposes was used to classify the gold mill tailings. The mill tailings were

classified as coarse-grained soil with 76.25% retained mass on the no. 200 sieve. Since the sample contains more than 12% fines, with 23.75% passing no. 200 sieve, it was classified as sand with fines. The liquid limit (LL), plastic limit (PL), and plasticity index (PI) were determined to be 20, 19, and 1, respectively. Using the plasticity chart, the samples were identified to be ML or silt. Thus, the gold mill tailings were classified as silty sand. Minerals in the gold mill tailing samples were cross-referenced to the RRUFF Project website (rruff.info), containing an integrated database of Raman spectra, XRD, and mineral chemistry data.

Figure 2 shows the XRD results, with the samples' major peaks identified as minerals. Mineral characterization showed that phyllosilicates and aluminosilicates were present in the gold mill tailings. This finding indicates that the gold mill tailings samples contain alumina and silica species dissolved by the alkali-activator to form oligomers. Based on the results, we hypothesize that, similar to the study of Zhang et al. (2011), the samples underwent polycondensation to form inorganic polymeric material and bonded to the undissolved solid particles of the source material in the final geopolymeric structure.

3.2 Strength development

Forty-eight (48) geopolymer specimens were loaded to failure using Unconfined Compression Test (UCT) by Instron 3366 universal testing machine. The highest compressive strength was observed at test case B2 with 10 M NaOH (0.3) alkali-activator (ratio), 0.03 MPa forming pressure, 80 °C curing temperature, and aged for 28 days at an average UCS of 2262 kPa. However, the lowest was found at test case A1 geopolymer samples of 10 M NaOH alkali-activator,

0.03 MPa forming pressure, 60 °C curing temperature, and aged for 7 days at an average UCS of 734 kPa.

The development of strength over time in the geopolymer specimens was investigated as shown in Fig. 3. The results indicate that the strength of the samples increased with time, with a percentage increase ranging from 8.38 to 118.50%. The highest strength was recorded for the treatment case of 0.03 MPa, 80 °C geopolymer samples, which reached over 2000 kPa, with a strength of 2041 and 2262 kPa recorded after 7 and 28 days of curing, respectively. The greatest increase in strength was observed in the geopolymer samples formed at a pressure of 1.78 MPa and treated at a temperature of 60 °C, with its 28-day strength of 1409 kPa being more than twice its 7-day strength of 644.81 kPa. However, the strength increase in 0.03 MPa, 60 °C geopolymer samples was only 8.38%, indicating that its ultimate strength may have been reached before 28 days. These results are comparable to those of geopolymerized copper tailings prepared using 11 M NaOH and cured at a temperature of 35 °C, as reported in the study of Manjarrez et al. (2018). In that study, the compressive strength of tailings with a moisture content of 16–19% was less than 1000 kPa and reached 3000 kPa for a moisture content of 14%.

The same increasing trend can be seen in Ca(OH)₂ geopolymer samples, but the percent increase was generally lower (0.27 to 37.31%) compared to NaOH geopolymer samples. The lowest percent increase of only 0.27% was from 0.03 MPa, 80 °C geopolymer samples. With almost zero increase in strength, this observation may be due to the ultimate strength of Ca(OH)₂ geopolymer samples being already reached at an earlier age, in this case, on its seventh day. However, it was evident that the geopolymer samples' strengths increased over time. Compressive strengths were also lower than NaOH geopolymer samples, with the highest strength recorded at only 1126.22 kPa for 1.78 MPa, 60 °C, 28-day geopolymer samples. However, this finding is marginally greater than the geopolymer produced from Zn tailings, which had a compressive strength of 1.1 MPa, reported in the study by Wan et al. (2019). A two-sample *t*-test on the strength development of geopolymer samples from 7 to 28 days showed a significant statistical difference ($p = 0.039, < 0.05$). This indicates that curing age affects the strength development of the geopolymer samples. A longer curing period produced geopolymer samples with higher strength. This may be due to the longer time for the aluminum silicates to form the three-dimensional geopolymeric framework with a sufficiently interconnected network of bonds. Consistent with the findings of the previous studies (Ahmari et al. 2012; Ren et al. 2015), this behavior is simply attributable to the effect of NaOH concentration on the dissolution of silica and alumina species and the polycondensation process.

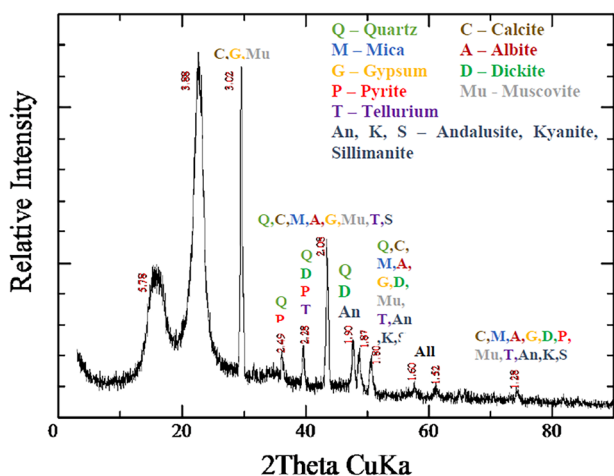
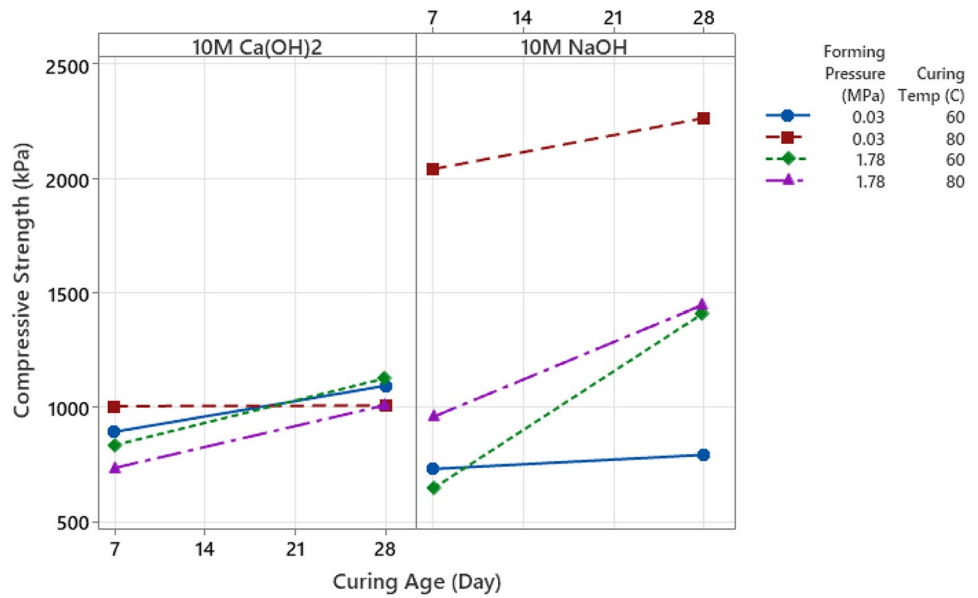


Fig. 2 XRD analysis results of the mill tailings samples

Fig. 3 Strength development of geopolymer samples after 7 and 28 days of curing for various treatment conditions



The compressive strength values were compared with various standards to determine the potential application of the produced geopolymer mill tailings based on their unconfined compressive strength. It was found that most of the test cases have applications for subgrade for road construction applications. The summary of potential applications is shown in Table 2.

3.2.1 Effect of curing temperature

Figure 4a displays a bar graph comparing the strength of geopolymer samples cured at 60 and 80 °C for a 28-day curing period. The results indicate that the majority of the samples cured at 80 °C exhibit higher strengths compared to those cured at 60 °C, with a few exceptions, such as the Ca(OH)₂, 1.78 MPa, 7-day and 28-day geopolymer samples and the Ca(OH)₂, 0.03 MPa, 28-day geopolymer samples. The average compressive strength of the geopolymer samples cured at 60 °C was 941 kPa, while the 80 °C cured samples had an average compressive strength of 1308 kPa. This study’s results align with the optimal temperature previously reported in the literature. For instance, Falayi (2019) found

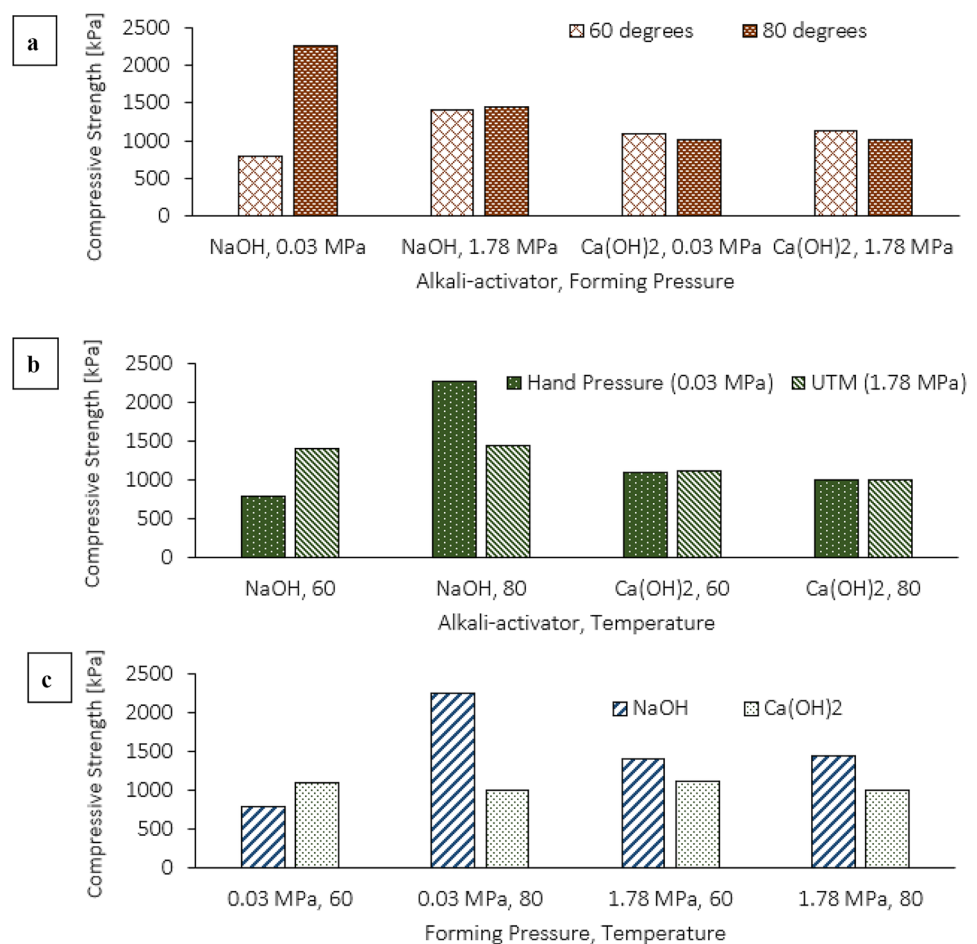
that 80 °C was the optimal temperature for activating geopolymer gold mill tailings with potassium silicate (KS) and potassium aluminate (KA). The improvement in strength was attributed to the increased dissolution of alumina and silica species, which added energy to the process. Similarly, Tian et al. (2020) observed that the compressive strength of copper tailings increased between 22 and 80 °C due to the homogeneous dissolution of aluminosilicate, leading to the formation of N–A–S–H and C–S–H gels. These gels had a positive impact on compressive strength. Both Falayi (2019) and Tian et al. (2020) concurred that temperatures above 80 °C would negatively impact the strength of geopolymer samples.

The paired *t*-test indicated a significant difference ($p = 0.015, < 0.05$) in the compressive strengths of the geopolymer samples cured at 60 and 80 °C. The increased curing temperature led to a corresponding increase in the compressive strength of the geopolymer samples. The temperature of 80 °C was found to be optimal, as it facilitated the polycondensation process while avoiding the formation of amorphous or crystalline materials that could negatively impact the dissolution of alumina and silica. Additionally, this temperature provided the necessary conditions for the gradual evaporation

Table 2 Potential application of geopolymer from gold mill tailings

Application	Minimum strength requirement (MPa)	Standard/reference	Test cases passing (applicable)
Medium to high volume subbase	2.068	Portland Cement Association (Portland Cement Association 1992)	B2
Subgrade	0.7	US Federal Highway Administration (Christopher et al. 2006)	All cases except C1
Subgrade, lightly bound pavement materials	1.0	Austrroads (Jameson 2019)	B1, B2, C2 D2, E2, F1, F2, G2, H2

Fig. 4 Effect of **a** temperature, **b** forming pressure, and **c** alkali-activator on the compressive strength of 28-day geopolymer samples



of water in the geopolymer samples, which was essential to complete the geopolymerization process.

3.2.2 Effect of forming pressure

Figure 4b shows the differences in geopolymer samples formed at different pressures of 0.03 and 1.78 MPa for 28-day geopolymers. The average compressive strength of 0.03 MPa geopolymer samples was 1229 kPa, while the average compressive strength of 1.78 MPa geopolymer samples was 1020 kPa. The difference between the two seemed small, as seen on the bar graph representations. For the 7-day geopolymer samples, lower forming pressure gave higher compressive strength. However, no general trend can be observed in 28-day geopolymer samples, with some geopolymer samples exhibiting higher compressive strengths for higher forming pressure. A paired *t*-test showed no statistically significant difference in the compressive strengths of the geopolymer samples ($p = 0.09$) at 5% significance.

Interestingly, the results indicate that the geopolymer samples formed at a higher pressure of 1.78 MPa had lower compressive strengths than those formed at a pressure of 0.03 MPa. This discrepancy could be attributed to the excessive expulsion

of alkali-activator solution, which resulted in a large portion of the alumina and silica species in the source material remaining unreacted. Furthermore, the 1.78 MPa pressure may have exceeded the optimal pressure necessary for the particles of the geopolymer paste to rearrange and form a denser structure. The beneficial impact of increased forming pressure with strength has been reported by Ahmari and Zhang (2013). Furthermore, based on the statistical analysis, the two forming pressures showed insignificant differences in the compressive strengths of the produced geopolymer samples. The optimum forming pressure might be between 0.03 and 1.78 MPa or lower than 0.03 MPa since most geopolymer specimens have shown lower compressive strengths for higher forming pressure. Other forming pressures and applications of it may be evaluated for further research in this study.

3.2.3 Effect of alkali-activator

The differences between NaOH and Ca(OH)₂ solutions in terms of their effect on the compressive strength of 28-day geopolymer samples are presented in Fig. 4c. Although the average compressive strength of NaOH geopolymer samples (1286 kPa) was higher than that of Ca(OH)₂ geopolymer

samples (963 kPa), this was not a universal trend, as depicted by the bar graph. For instance, at a forming pressure of 0.03 MPa, a curing temperature of 60 °C, and curing age of 28 days, the compressive strength of Ca(OH)₂ geopolymer samples was greater than that of NaOH geopolymer samples. On the other hand, the difference in strength between NaOH and Ca(OH)₂ geopolymer samples was more pronounced for some NaOH geopolymer samples, particularly those that were treated with 0.03 MPa and 80 °C and cured for 7 days or 28 days.

Paired *t*-test results show a significant difference in the compressive strength of the different alkali-activator solutions used ($p=0.019, <0.05$). We hypothesize that the 10 M NaOH alkali-activator dissolved more alumina and silica components, leading to a thicker geopolymeric binder and resulting in higher compressive strength. On the other hand, the 10 M Ca(OH)₂ alkali activator yielded geopolymer samples with lower compressive strengths as the additional lime in the geopolymer disrupted the optimal geopolymer gel binder structure, thus deterring the strength development.

3.2.4 Interaction of factors

The purpose of conducting an analysis of variance (ANOVA) in this study was to identify the optimal test case in the design

of geopolymer bricks. ANOVA was used to evaluate the reliability of the results and determine the means and impact of multiple factors through comparison. The results of the ANOVA were presented through a combination of graphical representation, including main effects and interaction plots, and quantitative analysis using a general linear model. The quantitative analysis was used to determine the significance of individual factors and their interactions (combined effects).

The main effect plots highlight the impact of the factors considered in this study on the mean values of compressive strength (Yong-Jie et al. 2023). These plots are essential because they help understand the influence of these factors on the compressive strength of geopolymer brick samples. The results indicate that, in general, the activator, curing temperature, and curing age have a positive effect on compressive strength, while forming pressure has an opposite effect, as shown in Fig. 5a. The interaction plots in Fig. 5b display the mean values for compressive strength, influenced by the type of activator, forming pressure, curing temperature, and curing age. Parallel lines in the interaction plots suggest that there is no interaction effect between the factors. The figure shows that most factors generally interact with each other, but the minimal interaction is with temperature and curing age.

Fig. 5 Effects of activator, forming pressure, curing temperature, and curing time on compressive strength of geopolymer concrete: **a** main effects and **b** interaction plots

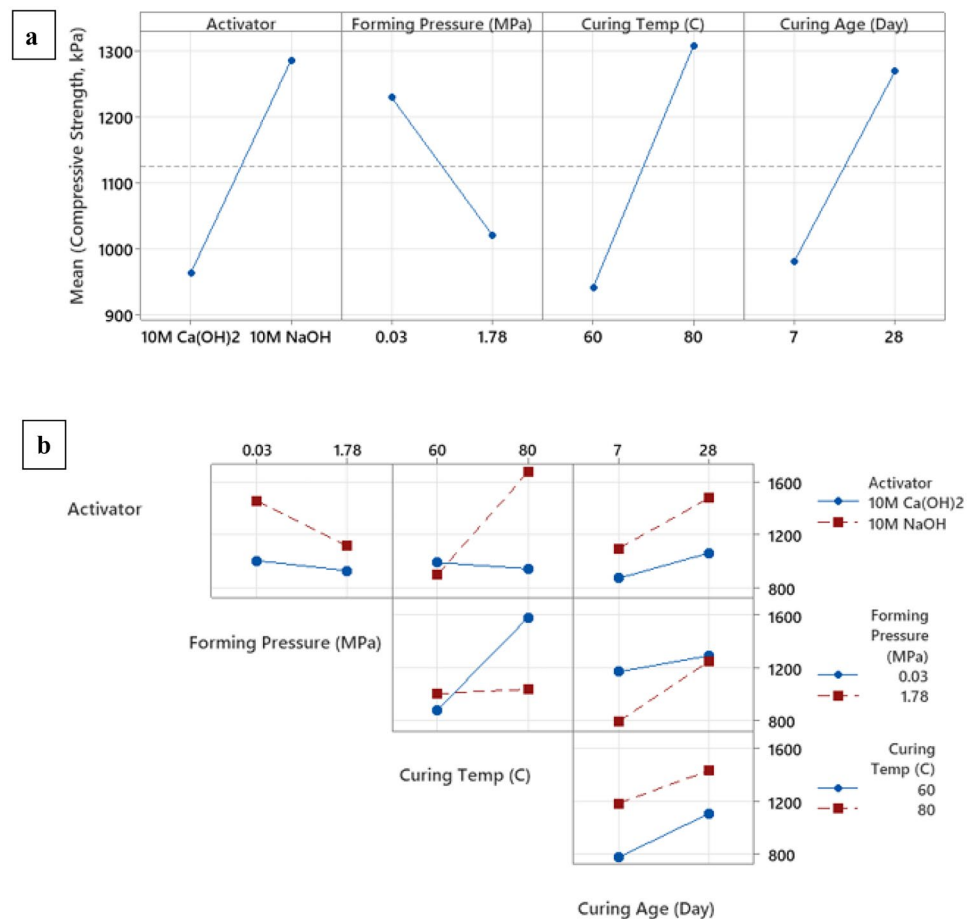


Table 3 ANOVA results for significance of each factor and interaction of factors

Factor/interaction	F-value	P-value
Age	19.31	0.000
Alkali activator	24.19	0.000
Forming pressure	10.16	0.003
Curing temperature	31.23	0.000
Age*alkali activator	2.12	0.155
Age*forming pressure	6.44	0.016
Age*curing temperature	0.4	0.530
Alkali activator*forming pressure	4.17	0.050
Alkali activator*curing temperature	40.05	0.000
Forming pressure*curing temperature	25.81	0.000
Age*alkali activator*forming pressure	1.34	0.256
Age*alkali activator*curing temperature	0.04	0.848
Age*forming pressure*curing temperature	0.24	0.630
Alkali activator*forming pressure*curing temperature	17.35	0.000
Age*alkali activator*forming pressure*curing temperature	1.38	0.249

The results of ANOVA on the significance of each factor and their combinations (interaction) using a general linear model are listed in Table 3. It enumerates the corresponding F statistic and p-values for different interactions of the four factors up to the highest 4-factor interaction effect. At a 5% level of significance, the 4-factor interaction effect and most of the 3-factor interaction effects, such as *age*alkali_activator*forming_pressure*, *age*alkali_activator*curing_temperature*, and *age*forming_pressure*curing_temperature*, were found to be insignificant ($p > 0.05$). It can be observed that most of the factors that resulted in insignificant differences were combined with the factor of “age.” The optimal treatment combination was determined to be TC2 with NaOH, 0.03 MPa, and 80 °C bricks, as shown in the boxplot of compressive strength vs. TC in Fig. 6. Since the effect of curing age was insignificant, the production of geopolymer bricks using the above-mentioned

optimal combination is cost-effective, as a shorter curing span and lower forming pressure can be applied without compromising the compressive strength of the produced geopolymer bricks. This also suggests that geopolymerization is a rapid process, consistent with the findings of Tian et al. (2020).

3.3 Durability performance

The average weight loss in percentage was calculated to determine geopolymer samples' durability when immersed in an acidic condition. A negative weight loss signifies a gain in weight. The results are tabulated in Table 4. The average weight loss of NaOH geopolymer samples ranged from 14.69 to 67.28%, averaging 36.46%. This was due to the strong acid and strong base reaction, where an exothermic condition was produced with sodium sulfate aqueous solution.

Fig. 6 Boxplot of compressive strength for different treatment combinations

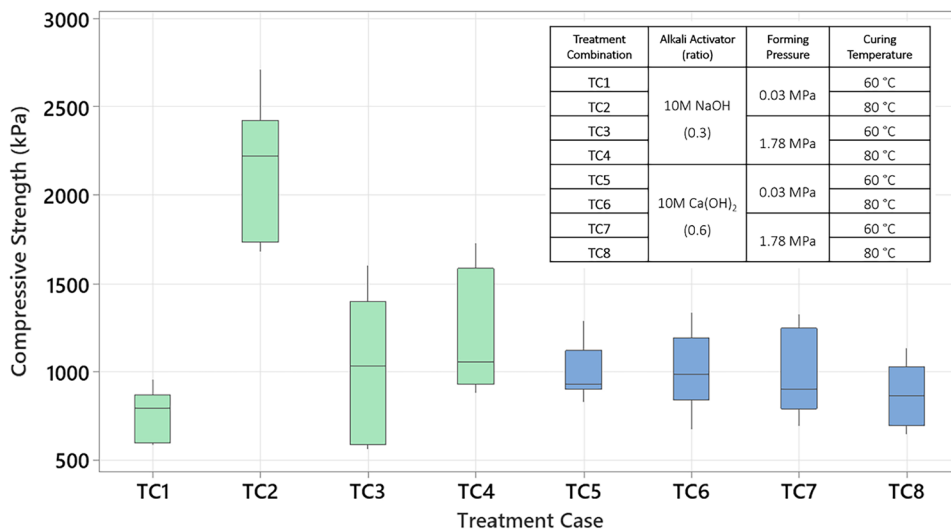


Table 4 Acid immersion test results

Alkali activator (ratio)	Forming pressure	Curing temperature	Initial mass (g)	Final mass (g)	Mass loss (%)	Average mass loss (%)	
10 M NaOH (0.3)	Hand pressure (0.03 MPa)	60 °C	219	67	69.41	67.28	
			219	87	60.27		
			221	61.5	72.17		
		80 °C	227.5	185	18.68		14.69
			224	198	11.61		
			225	194	13.78		
	Ultimate testing machine (1.78 MPa)	60 °C	219	147	32.88	36.17	
			224	134.5	39.96		
			220	141.5	35.68		
		80 °C	221.5	174.5	21.22		27.70
			224.5	157	30.07		
			220	150	31.82		
10 M Ca(OH)₂ (0.6)	Hand pressure (0.03)	60 °C	191	226	-18.32	-19.49	
			188	225.5	-19.95		
			188	226	-20.21		
		80 °C	195	217	-11.28		-14.40
			192	224.5	-16.93		
			193.5	222.5	-14.99		
	Ultimate testing machine (1.78)	60 °C	193	226	-17.10	-20.74	
			193	233.5	-20.98		
			190.5	236.5	-24.15		
		80 °C	197	229.5	-16.50		-14.75
			194.5	231.5	-19.02		
			195	212	-8.72		

The chemical reaction $2 \text{NaOH}_{(\text{aq})} + \text{H}_2\text{SO}_{4(\text{aq})} \rightarrow \text{Na}_2\text{SO}_{4(\text{aq})} + 2 \text{H}_2\text{O}_{(\text{l})}$ produced this result. However, $\text{Ca}(\text{OH})_2$ geopolymer samples showed an increase in mass after immersing them in an acidic condition, leading to an average weight gain of 17.35%. This was due to the formation of calcium sulfate precipitate upon reaction with sulfuric acid with the chemical reaction $\text{Ca}(\text{OH})_{2(\text{aq})} + \text{H}_2\text{SO}_{4(\text{aq})} \rightarrow \text{CaSO}_{4(\text{s})} + 2 \text{H}_2\text{O}_{(\text{l})}$.

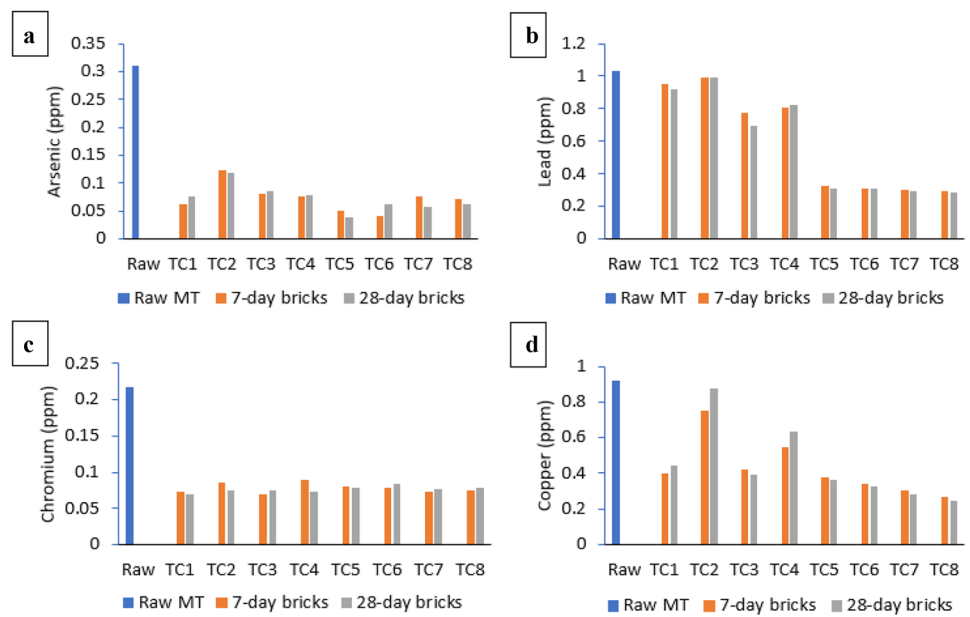
3.4 Heavy metals leaching potential

The concentration of several heavy metals, including arsenic, copper, cadmium, chromium, lead, and mercury, was quantified in raw gold mill tailings and geopolymer specimens using inductively coupled plasma–optical emission spectroscopy (ICP-OES). The leaching potential of the geopolymer specimens was evaluated by determining if the heavy metals from the source material were immobilized through the geopolymerization process. This was achieved by calculating the percent reduction in heavy metal concentration from the raw gold mill tailings to the resulting geopolymer specimens. The results, as illustrated in Fig. 7, demonstrate a significant reduction in heavy metal leaching as a result of the geopolymerization treatment of the raw

mill tailings. This reduction is further highlighted in Table 5, which displays the concentration of heavy metals in the raw gold mill tailings, the crushed geopolymer specimens, and the percent decrease in concentration from the raw material to the produced geopolymer samples.

The average decrease in arsenic concentration was 76.79%, ranging from 60 to 87%. The results indicate that the immobilization of arsenic was more effective in $\text{Ca}(\text{OH})_2$ geopolymer samples than in NaOH geopolymer samples, with an average decrease of 76.79 and 63.93%, respectively. Similarly, copper and cadmium concentrations showed a higher immobilization rate in $\text{Ca}(\text{OH})_2$ geopolymer samples, with average decreases of 52.69 and 33.35% compared to their corresponding NaOH geopolymer samples. The chromium concentration showed an average decrease of 64.63%. No specific pattern could be observed with regard to the factors affecting the leaching potential. The lead concentration showed a significant decrease in the $\text{Ca}(\text{OH})_2$ geopolymer samples, with an average decrease of 70%, while the NaOH geopolymer samples only showed an average decrease of 16%. The concentration of mercury was below the detection limit of the ICP-OES machine, which implies a 100% decrease from the raw gold mill tailings with 0.247 ppm mercury concentration.

Fig. 7 Heavy metal concentrations of raw and geopolymerized mill tailings for **a** arsenic, **b** lead, **c** chromium, and **d** copper



The decrease in heavy metal concentrations in the produced geopolymer samples demonstrates the efficacy of the geopolymerization process in immobilizing these metals and preventing their leaching. The greater decrease in heavy metal concentrations in the Ca(OH)₂ geopolymer samples suggests that this alkali activator was able to encapsulate a larger amount of heavy metals in its geopolymer matrix than the NaOH activator. This disparity may be attributed to the higher reactivity of Ca(OH)₂ with heavy metals, as well as the higher ratio of Ca(OH)₂ added to the source material (0.6 Ca(OH)₂/MT) compared to NaOH (0.3 NaOH/MT). These factors likely

led to the formation of more geopolymeric bonds, resulting in the trapping of a greater number of heavy metals.

To determine compliance with the US EPA standards, the maximum limit of heavy metal concentrations was compared to the levels present in the raw and geopolymerized mill tailings. The initial mercury concentration of the raw gold mill tailings was 0.247 ppm, which exceeded the US EPA’s maximum limit of 0.200 ppm. However, after geopolymerization, all specimens met the standards set by the US EPA for maximum heavy metal concentrations of arsenic, cadmium, chromium, lead, and mercury.

Table 5 Reduction in heavy metal leaching after geopolymerization

Alkali activator (ratio)	Forming pressure (MPa)	Curing temperature	Curing time (day)	% Difference with raw sample					
				As	Cu	Cd	Cr	Pb	Hg
	Concentration in raw sample (ppm)			0.31	0.92	0.22	0.22	1.04	0.25
10 M NaOH	0.03	60 °C	7	80.38	56.72	33.67	66.39	8.03	100.00*
			28	75.73	51.96	31.90	68.46	11.44	100.00*
	1.78	80 °C	7	60.35	18.35	33.40	60.97	4.50	100.00*
			28	62.31	4.47	32.95	66.02	3.99	100.00*
	0.03	60 °C	7	74.12	54.24	33.58	68.00	25.00	100.00*
			28	72.61	57.44	33.04	65.52	33.13	100.00*
1.78	80 °C	7	75.37	40.80	32.63	59.04	22.19	100.00*	
		28	74.99	31.08	32.58	66.25	20.24	100.00*	
10 M Ca(OH)₂	0.03	60 °C	7	84.14	59.22	33.76	62.90	68.96	100.00*
			28	87.29	60.89	33.81	63.91	69.98	100.00*
	1.78	80 °C	7	86.96	62.74	33.76	63.73	70.26	100.00*
			28	80.25	64.31	33.76	61.29	70.28	100.00*
	0.03	60 °C	7	75.28	67.04	33.49	66.30	71.25	100.00*
			28	81.80	69.82	33.72	64.97	72.07	100.00*
	1.78	80 °C	7	77.08	70.90	33.81	66.02	71.93	100.00*
			28	80.03	73.10	33.72	64.28	72.23	100.00*

4 Conclusions

Gold mill tailings with aluminosilicate minerals such as andalusite, kyanite, and sillimanite were used as the source material for geopolymerization. The compressive strength of the produced geopolymer was proportional to the curing age, with 28-day samples exhibiting higher strengths than 7-day samples. The optimal treatment for the highest compressive strength of 2.26 MPa involved a 10 M NaOH alkali-activator solution, 0.03 MPa forming pressure, and 80 °C curing temperature. The majority of the geopolymer samples from the mill tailings were deemed suitable for use as a subgrade for pavement applications based on their compressive strength. The curing temperature and alkali activator had a significant effect on the compressive strength, with a higher temperature and NaOH solution producing higher strengths. The effect of forming pressure was not significant. The geopolymerization process resulted in a decrease in heavy metal concentrations of arsenic, copper, cadmium, chromium, lead, and mercury, with calcium hydroxide geopolymer samples exhibiting a higher decrease than sodium hydroxide samples. The acid immersion test showed durable results for the Ca(OH)₂ geopolymer samples, with an average percent gain in mass, while the NaOH geopolymer samples showed drastic dissolution.

5 Recommendations

We recommend further research to broaden the application of this promising technology as follows:

- Investigate the impact of using a mixture of two source materials, including gold mine tailings, on the compressive strength of geopolymer bricks.
- Explore alternative forming conditions to enhance the compressive strength, durability, and leaching potential of the produced geopolymer bricks.
- Evaluate the effect of different alkali activators or combinations thereof on the properties of the geopolymer bricks.
- Assess the impact of curing time on the water absorption and durability of the produced geopolymer bricks.
- Conduct a field study to assess the performance of the geopolymer samples in actual construction applications.

Declarations

Conflict of interest The authors declare no competing interests.

References

Abdullah MMA, Ibrahim WMW, Tahir MFM (2015) The properties and durability of fly ash-based geopolymeric masonry bricks. In:

- Eco-efficient Masonry Bricks and Blocks: Design, Properties and Durability. Elsevier Inc., pp 273–287
- Adiansyah JS, Rosano M, Vink S, Keir G (2015) A framework for a sustainable approach to mine tailings management: disposal strategies. *J Clean Prod* 108:1050–1062. <https://doi.org/10.1016/j.jclepro.2015.07.139>
- Ahmari S, Zhang L (2013) Durability and leaching behavior of mine tailings-based geopolymer bricks. *Constr Build Mater* 44:743–750. <https://doi.org/10.1016/j.conbuildmat.2013.03.075>
- Ahmari S, Zhang L, Zhang J (2012) Effects of activator type/concentration and curing temperature on alkali-activated binder based on copper mine tailings. *J Mater Sci* 47:5933–5945. <https://doi.org/10.1007/s10853-012-6497-9>
- Amin M, Zeyad AM, Tayeh BA, Agwa IS (2021) Effect of high temperatures on mechanical, radiation attenuation and microstructure properties of heavyweight geopolymer concrete. *Struct Eng Mech* 80. <https://doi.org/10.12989/sem.2021.80.2.181>
- ASTM (American Society for Testing And Materials) (2014) ASTM D422–63 (Reapproved 2007)e2 Standard test method for particle-size analysis of soils 1. *J Test Eval*
- Bai Y, Guo W, Wang J et al (2022) Geopolymer bricks prepared by MSWI fly ash and other solid wastes: moulding pressure and curing method optimisation. *Chemosphere* 307:135987. <https://doi.org/10.1016/j.chemosphere.2022.135987>
- Behera SK, Mishra DP, Singh P et al (2021) Utilization of mill tailings, fly ash and slag as mine paste backfill material: review and future perspective. *Constr Build Mater* 309:125120. <https://doi.org/10.1016/j.conbuildmat.2021.125120>
- Brockenbrough RL, Editor P (2009) Highway engineering handbook building and rehabilitating the infrastructure: New York Chicago San Francisco Lisbon London Madrid Mexico City Milan New Delhi San Juan Seoul Singapore Sydney Toronto
- Cairncross KH, Tadie M (2022) Life cycle assessment as a design consideration for process development for value recovery from gold mine tailings. *Miner Eng* 183:107588. <https://doi.org/10.1016/j.mineng.2022.107588>
- Christopher BR, Schwartz C, Boudreau R (2006) Geotechnical aspects of pavements: reference manual. <https://www.fhwa.dot.gov/engineering/geotech/pubs/05037/05037.pdf>. Accessed 2 Aug 2022
- Corpus MPLJ, Rosei Monzon MT, Orozco CR, Germar FJ (2021) Effects and optimization of aggregate shape, size, and paste volume ratio of pervious concrete mixtures. *Philipp Eng J* 42:25–40
- Cox B, Innis S, Mortaza A et al (2022) A unified metric for costing tailings dams and the consequences for tailings management. *Resour Policy* 78:102862. <https://doi.org/10.1016/j.resourpol.2022.102862>
- Davidovits J (2002) Environmentally driven geopolymer cement applications. Geopolymer 2002 Conference, October 28–29, 2002, Melbourne, Australia. <https://www.geopolymer.org/wp-content/uploads/ENVIRONMENT.pdf>. Accessed 2 Aug 2022
- Falayi BT (2019) Effect of Potassium Silicate and Aluminate on the Stabilisation of Gold Mine Tailings. <https://doi.org/10.1680/jwarm.18.00015>
- Freidin C (2007) Cementless pressed blocks from waste products of coal-firing power station. *Constr Build Mater* 21. <https://doi.org/10.1016/j.conbuildmat.2005.08.002>
- Haigh S (2016) Consistency of the casagrande liquid limit test. *Geotech Test J* 39. <https://doi.org/10.1520/GTJ20150093>
- Jallu M, Asce SM, Saride S et al (2021) Effect of curing time on the performance of fly ash geopolymer-stabilized RAP bases. *J Mater Civ Eng* 33:04021001. [https://doi.org/10.1061/\(ASCE\)MT.1943-5533.0003581](https://doi.org/10.1061/(ASCE)MT.1943-5533.0003581)
- Jameson G (2019) Guide to pavement technology part 4D: stabilised materials. https://austroads.com.au/__data/assets/pdf_file/0033/179673/AGPT04D-19_Guide_to_Pavement_Technology_Part_4D_Stabilised_Materials.pdf. Accessed 2 Aug 2022

- Kesimal A, Yilmaz E, Ercikdi B (2004) Evaluation of paste backfill mixtures consisting of sulphide-rich mill tailings and varying cement contents. *Cem Concr Res* 34. <https://doi.org/10.1016/j.cemconres.2004.01.018>
- Khater HM (2012) Effect of calcium on geopolymerization of aluminosilicate wastes. *J Mater Civ Eng* 24. [https://doi.org/10.1061/\(asce\)mt.1943-5533.0000352](https://doi.org/10.1061/(asce)mt.1943-5533.0000352)
- Kiventerä J, Golek L, Yliniemi J et al (2016) Utilization of sulphidic tailings from gold mine as a raw material in geopolymerization. *Int J Miner Process* 149. <https://doi.org/10.1016/j.minpro.2016.02.012>
- Leong HY, Ong DEL, Sanjayan JG, Nazari A (2018) Strength development of soil–fly ash geopolymer: assessment of soil, fly ash, alkali activators, and water. *J Mater Civ Eng* 30. [https://doi.org/10.1061/\(asce\)mt.1943-5533.0002363](https://doi.org/10.1061/(asce)mt.1943-5533.0002363)
- Li Y, Shen J, Lin H et al (2022) Properties and environmental assessment of eco-friendly brick powder geopolymer binders with varied alkali dosage. *J Build Eng* 58:105020. <https://doi.org/10.1016/J.JOBE.2022.105020>
- Macasieb RQ, Orozco CR, Resurreccion AC (2021a) Heavy metal contamination assessment and source apportionment analysis using multivariate methods in surface sediments of mining-impacted rivers in Benguet. *Int J Environ Stud* 78:283–300. <https://doi.org/10.1080/00207233.2020.1802953>
- Macasieb RQ, Orozco CR, Resurreccion AC (2021b) Us epa wasp for transport modelling of mercury in the mining-impacted ambalanga river. *ASEAN Eng J* 11. <https://doi.org/10.11113/AEJ.V11.17052>
- Manjarrez L, Zhang L, Asce M (2018) Utilization of Copper Mine Tailings as Road Base Construction Material through Geopolymerization. [https://doi.org/10.1061/\(ASCE\)MT.1943-5533.0002397](https://doi.org/10.1061/(ASCE)MT.1943-5533.0002397)
- Nawaz M, Heitor A, Sivakumar M (2020) Geopolymers in construction - recent developments. *Constr Build Mater* 260:120472
- Opiso EM, Tabelin CB, Maestre CV et al (2021) Synthesis and characterization of coal fly ash and palm oil fuel ash modified artisanal and small-scale gold mine (ASGM) tailings based geopolymer using sugar mill lime sludge as Ca-based activator. *Heliyon* 7:e06654. <https://doi.org/10.1016/J.HELIYON.2021.E06654>
- Orozco CR, Urbino IJA (2022) Self-healing of cracks in concrete using Bacillus cibi with different encapsulation techniques. *J Eng Technol Sci* 54:220305–220305. <https://doi.org/10.5614/J.ENG.TECHNOL.SCI.2022.54.3.5>
- Petrillo A, Cioffi R, Ferone C et al (2016) Eco-sustainable geopolymer concrete blocks production process. *Agric Agric Sci Procedia* 8. <https://doi.org/10.1016/j.aaspro.2016.02.037>
- Portland Cement Association (1992) Portland Cement Association: soil-cement laboratory handbook. https://www.cement.org/docs/default-source/th-paving-pdfs/soil_cement/eb003.pdf?sfvrsn=2. Accessed 3 Jul 2021
- Qaidi SMA, Tayeh BA, Ahmed HU, Emad W (2022a) A review of the sustainable utilisation of red mud and fly ash for the production of geopolymer composites. *Constr Build Mater* 350:128892. <https://doi.org/10.1016/J.CONBUILDMAT.2022.128892>
- Qaidi SMA, Tayeh BA, Zeyad AM et al (2022b) Recycling of mine tailings for the geopolymers production: a systematic review. *Case Stud Constr Mater* 16:e00933. <https://doi.org/10.1016/j.cscm.2022.e00933>
- Qian L, Lin H, Li B, Dong Y (2023) Physicochemical characteristics and microbial communities of rhizosphere in complex amendment-assisted soilless revegetation of gold mine tailings. *Chemosphere* 320:138052. <https://doi.org/10.1016/J.CHEMOSPHERE.2023.138052>
- Ren X, Zhang L, Ramey D et al (2015) Utilization of aluminum sludge (AS) to enhance mine tailings-based geopolymer. *J Mater Sci* 50:1370–1381. <https://doi.org/10.1007/S10853-014-8697-Y/FIGURES/11>
- Saif MS, El-Hariri MOR, Sarie-Eldin AI et al (2022) Impact of Ca+ content and curing condition on durability performance of metakaolin-based geopolymer mortars. *Case Stud Constr Mater* 16. <https://doi.org/10.1016/j.cscm.2022.e00922>
- Sheikhhosseini Lori I, Toufigh MM, Toufigh V (2021) Improvement of poorly graded sandy soil by using copper mine tailing dam sediments-based geopolymer and silica fume. *Constr Build Mater* 281:122591. <https://doi.org/10.1016/j.conbuildmat.2021.122591>
- Shi B, Li X, Hu W et al (2023) Environmental risk of tailings pond leachate pollution: traceable strategy for leakage channel and influence range of leachate. *J Environ Manage* 331:117341. <https://doi.org/10.1016/J.JENVMAN.2023.117341>
- Silva Rotta LH, Alcântara E, Park E et al (2020) The 2019 Brumadinho tailings dam collapse: possible cause and impacts of the worst human and environmental disaster in Brazil. *Int J Appl Earth Obs Geoinf* 90:102119. <https://doi.org/10.1016/J.JAG.2020.102119>
- Sindhunata, Van Deventer JSJ, Lukey GC, Xu H (2006) Effect of curing temperature and silicate concentration on fly-ash-based geopolymerization. *Ind Eng Chem Res* 45. <https://doi.org/10.1021/ie051251p>
- Tayeh BA, Zeyad AM, Agwa IS, Amin M (2021) Effect of elevated temperatures on mechanical properties of lightweight geopolymer concrete. *Case Stud Constr Mater* 15:e00673. <https://doi.org/10.1016/J.CSCM.2021.E00673>
- Tian Q, Sasaki K (2021) Structural characterizations of fly ash-based geopolymer after adsorption of various metal ions. *Environ Technol (United Kingdom)* 42. <https://doi.org/10.1080/09593330.2019.1649469>
- Tian X, Xu W, Song S et al (2020) Effects of curing temperature on the compressive strength and microstructure of copper tailing-based geopolymers. *Chemosphere* 253:126754. <https://doi.org/10.1016/J.CHEMOSPHERE.2020.126754>
- Wan Q, Rao F, Song S, Zhang Y (2019) Immobilization forms of ZnO in the solidification/stabilization (S/S) of a zinc mine tailing through geopolymerization. *J Mater Res Technol* 8:5728–5735. <https://doi.org/10.1016/J.JMRT.2019.09.040>
- Xiaolong Z, Shiyu Z, Hui L, Yingliang Z (2021) Disposal of mine tailings via geopolymerization. *J Clean Prod* 284:124756. <https://doi.org/10.1016/J.JCLEPRO.2020.124756>
- Yong-Jie H, Cheng-Yong H, Yun-Ming L et al (2023) Strength optimization and key factors correlation of one-part fly ash/ladle furnace slag (FA/LFS) geopolymer using statistical approach. *J Build Eng* 63:105480. <https://doi.org/10.1016/j.job.2022.105480>
- Zhang L (2013) Production of bricks from waste materials - a review. *Constr Build Mater* 47
- Zhang L, Ahmari S, Zhang J (2011) Synthesis and characterization of fly ash modified mine tailings-based geopolymers. *Constr Build Mater* 25. <https://doi.org/10.1016/j.conbuildmat.2011.04.005>

Publisher's Note Springer Nature remains neutral with regard to jurisdictional claims in published maps and institutional affiliations.

Springer Nature or its licensor (e.g. a society or other partner) holds exclusive rights to this article under a publishing agreement with the author(s) or other rightsholder(s); author self-archiving of the accepted manuscript version of this article is solely governed by the terms of such publishing agreement and applicable law.